Scientific Research Publishing

Open Journal of Applied Sciences, 2025, 15(8), 2229-2243
https://www.scirp.org/journal/ojapps
ISSN Online: 2165-3925
ISSN Print: 2165-3917

Thermophysical Characterisation of a Raw Earth Brick Stabilised by the Addition of Cow Bone Ash Use in Construction

Bonaventure D. Yassiri[1*], Abba Falama[1], Modjonda[1], Babe Colbert[1], Souaibou[1], Noël Djongyang[2*]

[1]Department of Civil Engineering, National Advanced School of Engineering of Maroua, Maroua, Cameroon
[2]Department of Renewable Energy, National Advanced School of Engineering of Maroua, Maroua, Cameroon
Email: *bonaventureyassiridounvang@gmail.com, *noeldjongyang@gmail.com

How to cite this paper: Yassiri, B.D., Falama, A., Modjonda, Colbert, B., Souai and Djongyang, N. (2025) Thermophysical Characterisation of a Raw Earth Brick Stabilised by the Addition of Cow Bone Ash Use in Construction. *Open Journal of Applied Sciences*, **15**, 2229-2243.
https://doi.org/10.4236/ojapps.2025.158147

Received: January 20, 2025
Accepted: June 30, 2025
Published: August 1, 2025

Abstract

Local materials have been attracting attention in many countries for some time now. The performance of these materials in terms of durability and resistance makes them an asset in the choice of building structures. This article is based on an experimental study of the thermophysical characterisation of a raw earth brick made from bovine bone ash. We chose clay-based raw earth from the locality of Pitoa-Sonayo in the North Cameroon Region. Thermal effusivity, volumetric heat capacity and thermal conductivity were studied. The acronym Pitoa-Sonayo (PS) is used to represent the Pitoa-Sonayo samples. The laboratory results gave a thermal conductivity of 0.46. An average of 0.81% was obtained for the 0% added bovine ash content; 0.65% for the 2% content; 0.58% for the 4% content; 0.52% for the 6% content and 0.47% for the 8% content. Thermal effusivity ranged from 651.23 to 761.30. These results obtained in relation to the tests carried out show that the thermophysical characterisations carried out make it possible to specify the optimum conditions for using these raw earth briquettes and guarantee energy savings and respect for the environment.

Keywords

Thermophysical Characterization, Thermal Effusivity, Volumetric Heat Capacity, Thermal Conductivity

1. Introduction

In recent years, mankind's technological growth has led to the development of several varieties of raw earth building materials, both in developing and industrialized countries. The use of earth in construction, its availability and accessibility

is a factor that makes its use possible. The development of construction infrastructures in the northern zone is a major asset for the development of Cameroon, but this development in the building sector has a profound impact on housing (thermal comfort) and the environment. The use of cement, concrete and steel accounts for a significant proportion of energy consumption for building operations, combined with the rising cost of energy in general [1] [2]. Today, the world is focusing much more on the problem of heat exchange between premises and the environment. This vast and complex problem depends on a number of parameters, such as [3]:

- ✓ The nature of the materials used in construction.
- ✓ The shape of buildings, which influences the capture of solar energy.
- ✓ The climatic environment in which the building is located.
- ✓ The intersection of the ground.

Carbon dioxide emissions in the building sector now rank it among the most polluting sectors in the world, and it is the second biggest emitter of carbon dioxide after industry [4]. Studies by [5] [6], as a result, greenhouse gases are responsible for over 40% of global warming [7] [8]. This phenomenon is prompting global concerns about environmental and energy management to lead to rapid growth, with the need to build more energy-efficient sustainable housing and use natural resources as much as possible, according to Donatien René Riantsoa [9]. Earth offers enormous advantages in terms of thermal insulation [10], as well as social and cultural benefits, enabling people in Sudano-Sahelian regions to better cope with the high temperatures and heat waves that are becoming increasingly frequent with climate change. For many Sudano-Sahelian regions, earthen housing remains the only logically and reasonably feasible construction method, as they do not have sufficient material resources or the means to acquire and build housing for their inhabitants [11]. However, the new constructions take two factors into account: on the one hand, the durability of the construction, and on the other, the cost in relation to the existing [12]. The northern regions of Cameroon, characterized by a very hot, dry climate, face a number of problems in terms of housing and construction [13]. The construction methods used do not meet the climatic requirements of these regions. The building materials used are often concrete or cementitious products such as cinder blocks, mortars and adobes, which have poor thermal and mechanical properties, whereas these regions have a number of local materials (clay, laterite, etc.) that have proven their thermal and mechanical efficiency in the past [14]. These cities are undergoing extremely rapid urban development. Depending on the needs normally expressed, construction costs in the current situation are becoming increasingly high [14]. The State of Cameroon, anxious to reduce these costs, is working to find solutions and is encouraging research into the use of local materials, which looks promising. But our researchers have not yet explored this field. The main reason is that their thermophysical properties are not always well known, particularly their hygrothermal behaviour, an important factor in occupant comfort [3]. This policy of fighting the

cost of building materials led to the creation of a public establishment in 1990, reorganized on October 17, 2018 by presidential decree No. 2018/594 and placed under the Ministry in charge of scientific research (MIPROMALO) [15]. The aim of this structure is to enhance the value of natural resources (local and innovative materials) in order to reduce construction costs and national equipment such as stabilized earth bricks and terracotta bricks with a view to improving the thermophysical properties of construction materials in the national territory. Faced with all the above, we set out to find solutions to the above-mentioned problems, by making mud bricks incorporating materials with low density and low thermal conductivity, so that the mud brick would meet these requirements. We chose to incorporate an organic material into the clay brick. The recycling of waste at the end of its cycle (bones) is a contribution to environmental protection and the sanitation of our urban spaces [16], as this waste abandoned in nature (restaurants, slaughterhouses and households) is a major source of waste [5] [15].

2. Presentation of the Study Area

Our study was carried out in the North Cameroon region, Bénoué Division, Pitoa Subdivision and Sonayo village (**Figure 1**) with geographical coordinates: 9˚36'0"N, 13˚26'24"E.

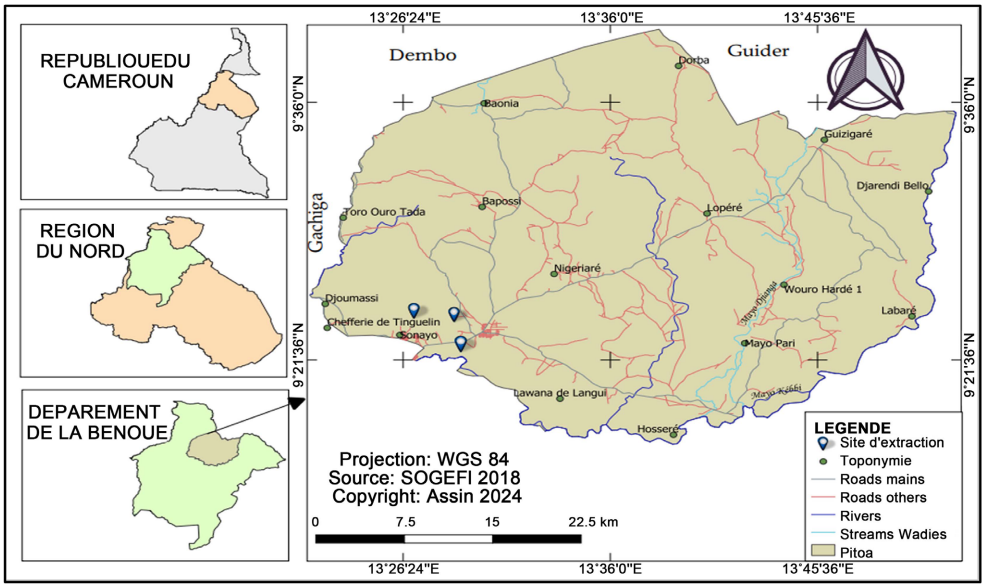

Figure 1. Location map of study area (North Cameroon).

3. Materials and Methods

3.1. Materials

As materials in this work we have Clay material (**Figure 2**), Organic material (**Figure 3**), Material sample (**Figure 4**), Asymmetric hot plane experimental set-up (**Figure 5**) and the Hot plane experimental set-up (**Figure 6**).

Figure 2. Clay material used.

Figure 3. Organic material.

Figure 4. Material sample.

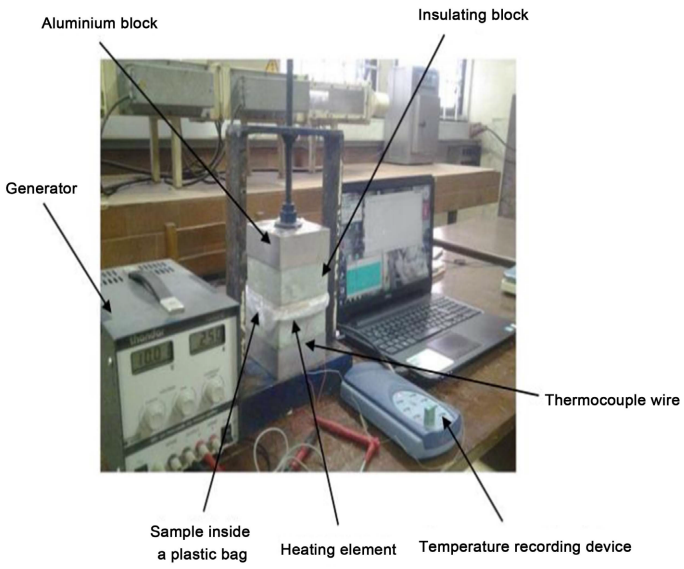

Figure 5. Asymmetric hot plane experimental set-up.

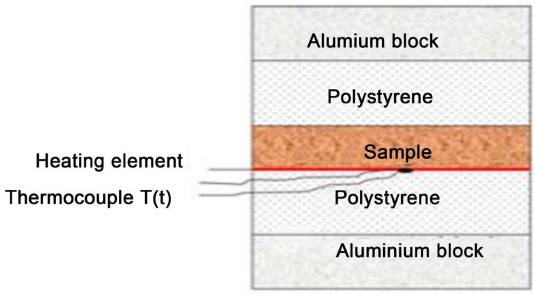

Figure 6. Hot plane experimental set-up.

3.2. Methods

The clay material (Figure 2) used to make the mud bricks comes from the North Cameroon region, Pitoa subdivion and Sonayo village is first dried, then ground by hand using a stone to obtain particles of a maximum size of 4 mm. The cow bones (Figure 3) are calcined at a temperature of 600 degrees celsus for 5 hours. After calcination the bones were ground in an electric grinder to obtain a powder size of 5 mm. Combinations were made with 0%, 2%, 4%, 6% and 8% by weight of cow bone ash. The clay is mixed with the bone ash at a time of 20 minutes using a percentage of 26% water per dry weight of earth until a homogeneous mixture is obtained. The clay paste is covered with plastic at room temperature for 24 days to promote the mixture (clay + bone ash) is placed in square moulds 10 × 10 × 3 cm^3 in three layers and each layer is pressed manually with twenty shocks and gradually another layer is added until the mould is filled after the last layer. The samples are kept in a chamber (22˚C ± 5˚C) in ambient air for 24 h with a humidity of 60% before being demoulded for drying. To carry out the various tests, the mud bricks are first left in the shade for a period of at least 21 days. Drying in the chamber is to prevent the clay bricks (Figure 5) from cracking and Figure 5 shows the asymmetric hot plane experimental set-up for thermal characterization.

Thermophysical Characterisation

Measuring equipment for estimating thermophysical parameters

A 10 × 10 × 3 cm^3 sample is placed on a heat sensor between two blocks of 10 × 10 × 3 polystyrene. The increase in temperature at the centre of the thermal resistance is the result of a type K thermocouple recording the test temperature on the hot surface of the material. Experimental temperatures Texp (t) were recorded using the TC 08-USB acquisition module. The experimental and simulated temperature drop obtained after modelling the test instrument helped us to estimate E and ρc_p. It is therefore important to note that the temperature above the polystyrene blocks remains at its initial state, to arrive at this point we placed two 10 × 10 × 3 aluminium blocks above and below the polystyrene blocks hblock = 10 W/m^2K; λblock = 200 W/mK, b = 100 mm, we find Bi = 0.005 which is well below 0.1.

a) Quadrupole models of the complete heat transfer model

Since the transverse dimensions of the resistor are larger than the thickness of the sample, heat transfer can be considered unidirectional at the center of the

probe, and modeled using the quadrupole method [12] [16] [17]. In this case, lateral convective losses h at the sides of the sample can be neglected. Secondly, we consider the probe as a thin system (the temperature will then be uniform over the entire thickness of the probe). The thermal quadrupole method applied to the sample for the upward flow is used to solve this problem and is written:

$$\begin{pmatrix} \theta_0 \\ \Phi_{01} \end{pmatrix} = [M_1][M_2][M_3] \tag{1}$$

$\theta_0 = L\left(T_0(x,t)\right)$: The Laplace transform of the temperature rise at the probe.

$\Phi_{01} = L\left(\phi_0(x,p)\right)$: The upward transform of the heat flux density dissipated in the sample.

M_1: The element representing the probe's half-thickness

$$[M_1] = \begin{pmatrix} 1 & 0 \\ \dfrac{m_s c_s}{S} p & 1 \end{pmatrix} = \begin{pmatrix} 1 & 0 \\ \rho_s c_s e_s p & 1 \end{pmatrix} \tag{2}$$

M_2: The element representing contact resistance at the probe-sample interface

$$[M_2] = \begin{pmatrix} 1 & SR_{cse} \\ 0 & 1 \end{pmatrix} \tag{3}$$

M_3: The element representing the material considered as semi-infinite

$$[M_3] = \begin{pmatrix} \theta_3 \\ E\sqrt{p}\theta_3 \end{pmatrix} \tag{4}$$

The quadrupole method applied to the downward flux is written by also considering the insulator as a semi-infinite material:

$$\begin{pmatrix} \theta_0 \\ \Phi_{02} \end{pmatrix} = [M_4][M_5] \tag{5}$$

Φ_{02}: The Laplace transform of the heat flux density dissipated downwards in the sample.

M_4: The element representing contact resistance at the probe-insulator interface

$$[M_4] = \begin{pmatrix} 1 & SR_{csi} \\ 0 & 1 \end{pmatrix} \tag{6}$$

M_5: The element representing contact resistance at the probe-insulator interface

$$[M_5] = \begin{pmatrix} \theta_4 \\ E_i\sqrt{p}\theta_4 \end{pmatrix} \tag{7}$$

The total flux density is given by:

$$\phi_0 = \phi_1 + \phi_2 \tag{8}$$

Combining all these different matrices, we arrive at the relationship that represents the theoretical response of the asymmetric semi-infinite hot plane model in

Laplace space:

$$\theta_{SI}(x,p)=\frac{\phi_0 S}{p}\cdot\frac{1}{\dfrac{\rho_s c_s e_s Sp+\left(1+R_{chs}\rho_s c_s e_s Sp\right)ES\sqrt{p}}{1+R_{chs}ES\sqrt{p}}+\dfrac{E_i S\sqrt{p}}{1+R_{chi}E_i S\sqrt{p}}} \tag{9}$$

$\theta_{SI}(x,p)$ the Laplace transform of the temperature at the center of the probe $T_{model\,SI}(x,t)=L^{-1}\left(\theta_{SI}(x,p)\right)$.

Using Stelfest's method [18] [19], the simplified long-time estimate (simplified model) of relation (9) gives the temperature evolution in real space at the center of the material.

$$\Delta T\left(0,t\to\infty\right)=\phi_0 S\left(\frac{E^2R_{chs}+E_i^2R_{chi}}{\left(E+E_i\right)^2}-\frac{\rho_s c_s e_s}{S\left(E+E_i\right)^2}\right)+\frac{2\phi_0}{\left(E+E_i\right)\cdot\sqrt{\pi}}\sqrt{t} \tag{10}$$

Numerical calculation of the slope $\alpha(t)=\dfrac{\Delta T\left(t+dt\right)-\Delta T\left(t\right)}{\sqrt{t+dt}-\sqrt{t}}$ of the curve $T=f\left(t^{1/2}\right)$, allows us to obtain a pre-estimate (preest) of the material's thermal effusivity, given by relationship (10).

$$E_{preest}=\frac{2\phi_0}{\alpha\sqrt{\pi}}-E_i \tag{11}$$

The volumetric heat capacity ρC_p can also be pre-estimated from the simplified model. Heat transfer through the probe over a time interval corresponds to an infinitely small heat $\rho_0=\dfrac{\delta q}{dt}$, which causes a temperature rise dT in the probe. By exploiting the linear part of the thermogram $T=f\left(t\right)$, we can numerically calculate its slope β and thus deduce the pre-estimated value of the sample's volumetric heat capacity by the relation

$$\left(\rho C_p\right)_{preest}=\frac{\dfrac{\phi_o}{\beta}-\rho C_{pi}e_i-\rho C_{ps}e_s}{e} \tag{12}$$

The pre-estimates of E and ρC_p will enable us to determine the apparent thermal conductivity of the materials using relationship (13).

$$\lambda_{preest}=\frac{\left(E^2\right)_{preest}}{\left(\rho C_p\right)_{preest}} \tag{13}$$

b) Asymmetrical 1D quadrupole models for the complete model

✓ Temperature at sensor center for complete model ($T_{model}(x,t)$)

Consider the diagram in **Figure 6**. Applying the quadrupole formalism, we have [8] [17]:

$$\begin{pmatrix}\theta_0\\ \Phi_{01}\end{pmatrix}=[M_1][M_2][M_6][M_7][M_8]\begin{pmatrix}\theta_5\\ \Phi_5\end{pmatrix}=\begin{pmatrix}A & B\\ C & D\end{pmatrix}\begin{pmatrix}\theta_5\\ \Phi_5\end{pmatrix} \tag{14}$$

M_6: The element representing the material to be characterized:

$$[M_6]=\begin{pmatrix} A_e & B_e \\ C_e & D_e \end{pmatrix} \tag{15}$$

$$A_e=\cosh(q_e\cdot e) \quad B_e=\frac{\sinh(q_e\cdot e)}{\lambda_e\cdot q_e} \quad q=\sqrt{\frac{p\rho C_p}{\lambda}} \tag{16}$$
$$C_e=\lambda_e\cdot q_e\cdot\sinh(q_e\cdot e) \quad D_e=A_e$$

M_7 : The element representing contact at the sample/insulator interface

$$[M_7]=\begin{pmatrix} 1 & SR_{cei} \\ 0 & 1 \end{pmatrix} \tag{17}$$

M_8 : The element representing the insulating material.

$$[M_8]=\begin{pmatrix} A_i & B_i \\ C_i & D_i \end{pmatrix} \tag{18}$$

With:

$$A_i=\cosh(q_i\cdot e_i) \quad B_i=\frac{\sinh(q_i\cdot e_i)}{\lambda_e\cdot q_i} \tag{19}$$
$$C_i=\lambda_i\cdot q_i\cdot\sinh(q_i\cdot e_i) \quad D_i=A_i$$

The role of the aluminum block here is to keep the temperature constant at the insulating material/aluminum block interface, and if we evaluate the Biot number of this block by the relation (20):

$$(Bi)_{bloc}=\frac{h_{bloc}\cdot b}{\lambda_{bloc}} \tag{20}$$

With values $h_{bloc}=10\ \mathrm{W/m^2\cdot K}$; $\lambda_{bloc}=200\ \mathrm{W/m\cdot K}$, $b=100\ \mathrm{mm}$, we find $Bi=0.005$ which is well below 0.1, in which case it can be considered uniform. Then let:

$$\theta_5(x,p)=L(\Delta T(x,p))_{bloc}=0$$
$$\theta_4(x,p)=L(\Delta T(x,p))_{bloc}=0 \tag{21}$$

In the same way, in Equation (2), the matrix element M_5 is replaced by the matrix M_8:

$$\begin{pmatrix} \theta_0 \\ \Phi_{02} \end{pmatrix}=[M_4][M_8]\begin{pmatrix} \theta_4 \\ \Phi_4 \end{pmatrix} \tag{22}$$

By combining relations (1), (11) and (18), we found the temperature at the centre of the probe in Laplace space, given by relation (22):

$$\theta_0(x,p)=\frac{\phi_0}{p}\cdot\frac{1}{\frac{D}{B}+\frac{D_i}{B_i+R_{csi}D_i}} \tag{23}$$

The Levenberg-Marquart (1944) algorithm integrated into a Matlab code can then be used to estimate the value of E that minimises the sum of the quadratic deviation errors of the ψ functional [12] [17].

$$\psi=\sum_{i=1}^{n}\left[\Delta T_{exp}(t_i)-T_{model}(t_i)\right]^2 \tag{24}$$

between the experimental curve $\Delta T_{exp}(t) = T(0,t) - T_a$ and the theoretical curve $T_{model}(x,t) = L^{-1}(\theta_0(x,p))$.

✓ Determination **of heat capacity (HC)**

Knowing the experimental density ρ_{exp} and estimating the volumetric heat capacity ρC_p, we can estimate the heat capacity C_p using the relationship:

$$C_p = \frac{(\rho C_p)_{modelcomplet}}{\rho_{exp}} \tag{25}$$

4. Results and Discussion

4.1. Specific Heat of Composite Material with Added Bone Centre

The specific heat C_{exp} is obtained from the heat capacity $(\rho C)_{exp}$ measured using the experimental hot plane and the density. Figure 7 illustrates the different values of the brick with the addition of bovine bone ash. The above results show that the variation of the effective temperature increases with the increase of the bone ash in the brick material.

These different results are 1033903.35; 1033364.69; 981369.638; 927856.381 and 890479.511 J/m³K with 0%, 2%, 4%, 6% and 8% addition of cow bone ash. The specific heat of an object or body is the energy required to increase the temperature of part of the object by 1 Kelvin, and we find a 13.87% difference in specific heat between real bricks and bricks containing 8% of cow bone ash. The decrease in the specific heat of an earth brick mixed with bone ash, as a function of percentage, is due to the change in the internal structure of the material and the variation in its capacity to store heat. The addition of bone ash, whose specific heat is generally lower than that of raw earth, reduces the overall capacity of the mixture to store heat. The less insulating the material. The specific heat and calorific value of an earth brick mixed with bone ash decrease as the percentage of bone ash increases, due to their intrinsic thermal properties [8] [12]. Bone ash generally has a lower specific heat and calorific value than raw earth. Therefore, adding bone ash reduces the brick's ability to store and release heat (Figure 7).

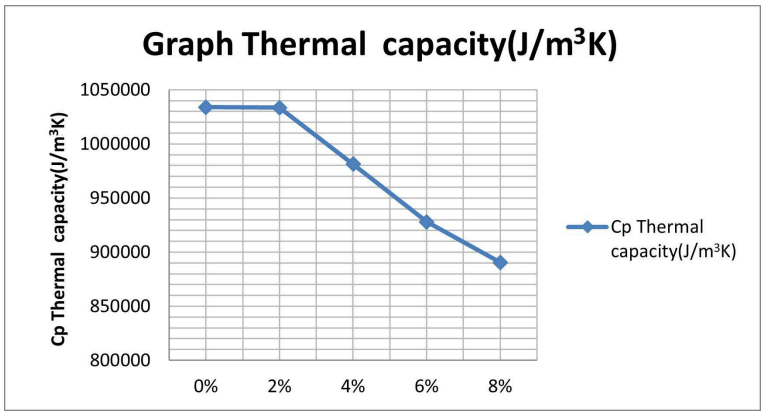

Figure 7. Volume heat capacity.

4.2. Thermal Effusivity

The thermal effusivity curve obtained shows how the variation in temperature increases with the rate of addition. On the other hand, the temperature of the insulating material also has a capacity to reduce thermal effusivity. Looking at the values on the histograms (Figure 8), we can see that the thermal effusivity of our material decreases with the addition of cow bone ash. The percentage difference is 12.08%, the thermal effusivity between the reference bricks (744.1056 $J/m^2Ks^{1/2}$) and that with the addition of 8% cow bone ash (654.1576 $J/m^2Ks^{1/2}$) obtained. This reduction is due to the presence of hollow pores in the cow bone ash, a function of the morphology or shape of the material.

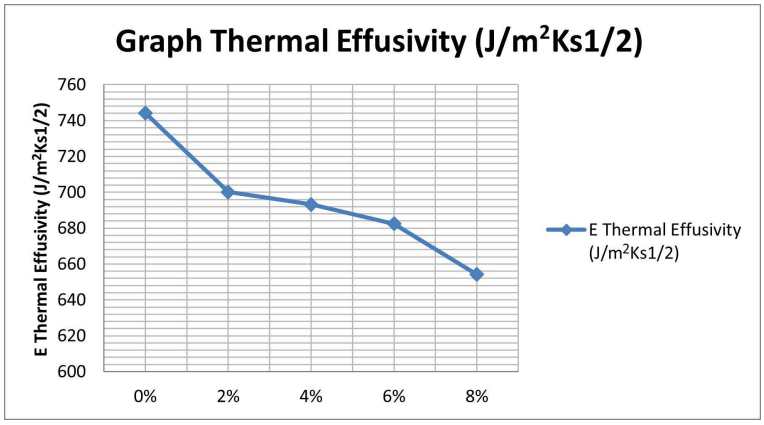

Figure 8. Thermal effusivity.

The percentage of organic matter added, the composition of the material and the porosity of the material all influence the thermal performance of the material [8] [17]. Table 1 shows the Thermal Properties of different materials.

Table 1. Thermal properties of different materials.

Samples	E Thermal Effusivity ($J/m^2Ks^{1/2}$)	C_p Thermal capacity (J/m^3K)	λ Thermal Conductivity (W/mK)	ρ Density (kg/m^3)
Brique + 0% de cendre	744.10565	1033903.35	0.81253	1536
Brique + 2% de cendre	700.095677	1033364.69	0.650024	1653
Brique + 4% de cendre	693.176319	981369.638	0.5850216	1436
Brique + 6% de cendre	682.410861	927856.381	0.52651944	1490
Brique + 8% de cendre	654.157647	890479.511	0.4738675	1591

4.3. Thermal Conductivity

This is the essential assessment of the energy performance that a material can deliver. Changes in thermal conductivity are a function of the percentage of additives (porosity of the raw materials) as shown in Figure 9. When organic matter is added, the thermal conductivity of the composite material decreases as

a function of the additives added. It decreases from 0.8 to 0.4 W/Km, *i.e.* a percentage decrease of 50%. A material is more insulating than a porous material. It has been concluded that this composite has very good thermal performance, making it suitable for use as a thermal insulation material. The addition of cow bone ash considerably reduces the thermal conductivity of the material due to the increase in porosity. In addition to the calcium sulphate in the cow bone meal, which acts as a natural cement, binding the particles of earth and sand together. This binding action strengthens the structure of the brick, improving its compressive strength and durability, which has a positive influence on its ability to manage heat exchange. Figure 9 shows the variation in porosity as a function of

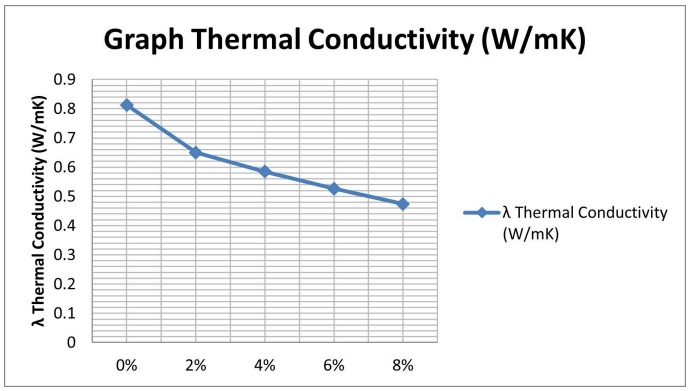

Figure 9. Changes in thermal conductivity as a function of ash content (%).

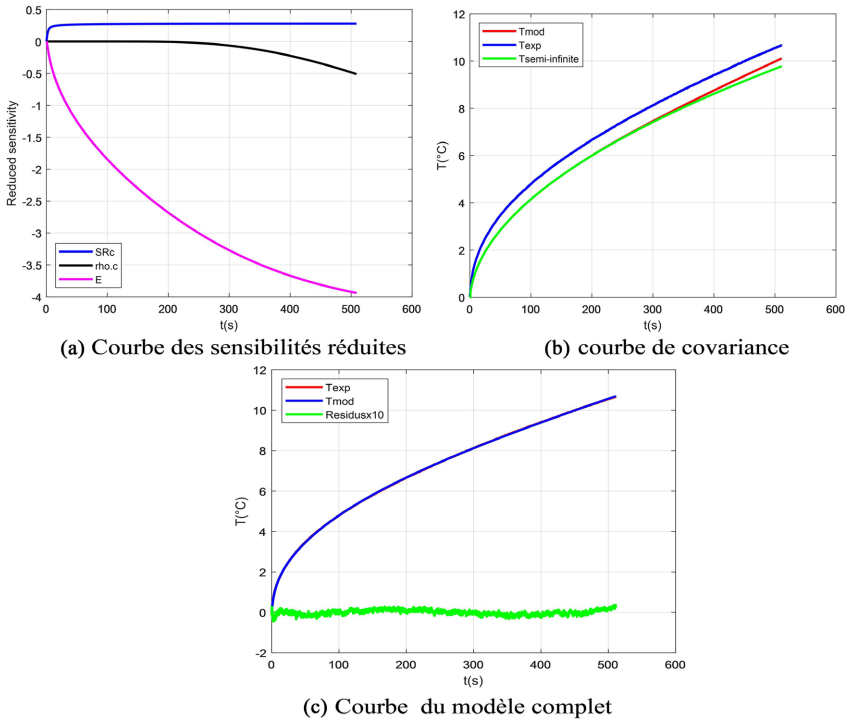

(a) Courbe des sensibilités réduites (b) courbe de covariance

(c) Courbe du modèle complet

Figure 10. Experimental curve of the complete hot plane model as a function of temperature and time obtained for a sample: (a) Curve of reduced sensitivities (b) Covariance curve; (c) Curve of the complete model [7] [12] [17].

the level of organic matter [16]. An increase in porosity reduces the proportion of clay material, ensuring heat diffusion within the products. Thermal diffusivity is reduced and, consequently, thermal conductivity. The lower thermal conductivity values are shown in the table above. Consequently, BTS with low thermal conductivity has pores in the material [11] [20]-[23].

The evolution between the experimental and theoretical curves is satisfactory, as shown by the curves estimating the covariance, sensitivity and residuals. This is why the thickness/width ratio always obeys the limits set in **Figure 10**, to keep the 1D transfer at the centre and the contact resistances negligible [8].

In general, earth bricks stabilised with cow bone ash from 2% regulate the thermal conductivity of the material and are more suitable for housing construction compared to earth bricks without the addition of ash, meanwhile, numerous researchers have proven that the addition of cow bone ash improves thermal properties, compressive strength and durability [3] [8] [21] [24]-[26].

5. Conclusion

This work consisted of an experimental study of the thermophysical characterisation of a raw earth brick based on cow bone ash. It is clear from this approach that sustainable development has the advantage of using raw materials which are renewable, ecological, resistant, durable and available. Furthermore, this work aims to contribute to the improvement of adobe manufacturing techniques using raw earth with the addition of cow bone ash. The adobes designed for this work were formulated from the raw earth mixture with contents of 0%, 2%, 4%, 6% and 8% respectively. The results show that our material has a thermal conductivity of 0.81 to 0.47 W/mK, which decreases with the addition of cow bone ash, with a fall rate of 60.6%, proving that the organic matter incorporated into the raw earth contributes to improving the thermal comfort of the building. The specific heat of an earth brick mixed with cow bone ash decreases as the percentage of bone ash increases the result values which are 1033903.35 to 890479.51 J/m^{3}K. This is because bone ash has a lower specific heat than earth. Adding bone ash therefore reduces the mixture's ability to store heat, which in turn reduces its calorific value. However, this mix can offer benefits in tropical and hot regions due to its ability to regulate temperature and humidity, improving thermal comfort. On the other hand, effusivity decreased with the addition of organic matter from 744.10 to 654.15 J/m^{2}Ks$^{1/2}$, with an average of 34.73%. This allows us to state that the composite obtained in this way is of particular interest in terms of thermal insulation in buildings, allowing it to be used in the construction sector. However, the best thermophysical behaviour is observed from proportions of 2% to 8% which means that it heats up and cools down more quickly. This is of great advantage for climates where the temperature sometimes reaches 45˚C in the shade, such as in the North region of Cameroon where this study is carried out to support sustainable living and construct houses resilient in the rural areas in opposition to the natural disasters and limit ventilation through household appliances in homes in order to reduce energy consumption.

Conflicts of Interest

The authors declare no conflicts of interest regarding the publication of this paper.

References

[1] Ahmad, T. and Zhang, D. (2020) A Critical Review of Comparative Global Historical Energy Consumption and Future Demand: The Story Told So Far. *Energy Reports*, **6**, 1973-1991. https://doi.org/10.1016/j.egyr.2020.07.020

[2] Geissler, S., Österreicher, D. and Macharm, E. (2018) Transition Towards Energy Efficiency: Developing the Nigerian Building Energy Efficiency Code. *Sustainability*, **10**, Article 2620. https://doi.org/10.3390/su10082620

[3] Meukam, P., Jannot, Y., Noumowe, A. and Kofane, T.C. (2004) Thermo Physical Characteristics of Economical Building Materials. *Construction and Building Materials*, **18**, 437-443. https://doi.org/10.1016/j.conbuildmat.2004.03.010

[4] Damfeu, J.C., Meukam, P. and Jannot, Y. (2016) Modeling and Measuring of the Thermal Properties of Insulating Vegetable Fibers by the Asymmetrical Hot Plate Method and the Radial Flux Method: Kapok, Coconut, Groundnut Shell Fiber and Rattan. *Thermochimica Acta*, **630**, 64-77. https://doi.org/10.1016/j.tca.2016.02.007

[5] Ouedraogo, M., Dao, K., Millogo, Y., Aubert, J., Messan, A., Seynou, M., *et al.* (2019) Physical, Thermal and Mechanical Properties of Adobes Stabilized with Fonio (*Digitaria exilis*) Straw. *Journal of Building Engineering*, **23**, 250-258. https://doi.org/10.1016/j.jobe.2019.02.005

[6] Babé, C., Yanné, E., Souaibou, Mojonda, Bakaiyang, L., Kola, B., *et al.* (2024) Thermophysical, Mechanical and Durability Characterization of Adobe Bricks Reinforced with Fonio (*Digitaria exilis*) Sounds. *Advances in Materials Physics and Chemistry*, **14**, 146-164. https://doi.org/10.4236/ampc.2024.148012

[7] Decret N090/1553 du 18 septembre 1990. Modifie et complete par le decret n02018/594 du 17 octobre 2018, qui a reoganise la MIPROMALO en tant qu'etablissement public a caractere scientifique, technique et professionnel.

[8] Modjonda, Souaibou, Etienne, Y. and Raidandi, D. (2023) Thermal and Mechanical Characterization of Compressed Clay Bricks Reinforced by Rice Husks for Optimizing Building in Sahelian Zone. *Advances in Materials Physics and Chemistry*, **13**, 177-196. https://doi.org/10.4236/ampc.2023.1310013

[9] Putri, E.R.M. and Surjanto, S.D. (2017) Performance of Gahver-Stehfest Numerical Laplace Inversion Method on Option Pricing Formulas. *International Journal of Computing Science and Applied Mathematics*, **3**, 71-76. https://doi.org/10.12962/j24775401.v3i2.2215

[10] Kola, B., Babé, C. and Djongyang, N. (2024) Thermophysical and Mechanical Characterization of the Earth-Straw Materials Employed in the Building of Shell Houses in the Mourla Region of Cameroon's Far North. *International Journal of Sustainable and Green Energy*, **13**, 43-57. https://doi.org/10.11648/j.ijrse.20241303.11

[11] Kitmo and Rahman, M.M. (2024) Investments in Energy Complexes: Evidence from Tajikistan. In: Dinçer, H., Yüksel, S. and Deveci, M., Eds., *Contributions to Management Science*, Springer, 209-219. https://doi.org/10.1007/978-3-031-51532-3_17

[12] Sathyapriya, G., Natarajan, U., Sureshkumar, B., Navaneethakrishnan, G., Palanisamy, R., Bajaj, M., *et al.* (2022) Quality and Tool Stability Improvement in Turning Operation Using Plastic Compliant Damper. *Journal of Nanomaterials*, **2022**, Article ID: 8654603. https://doi.org/10.1155/2022/8654603

[13] Deluxni, N., Sudhakaran, P., Kitmo and Ndiaye, M.F. (2023) A Review on Image En-

hancement and Restoration Techniques for Underwater Optical Imaging Applications. *IEEE Access*, **11**, 111715-111737. https://doi.org/10.1109/access.2023.3322153

[14] Minai, A.F., Khan, A.A., Kitmo, Ndiaye, M.F., Alam, T., Khargotra, R., *et al.* (2024) Evolution and Role of Virtual Power Plants: Market Strategy with Integration of Renewable Based Microgrids. *Energy Strategy Reviews*, **53**, Article 101390. https://doi.org/10.1016/j.esr.2024.101390

[15] Sahu, S.K., Mazumdar, K., Kitmo, Jember, Y.B. and Das, S. (2024) Design and Investigation of InGaAs/InP/InALAs MOSFET with Optimized Switching Efficiency. *IEEE Access*, **12**, 70045-70052. https://doi.org/10.1109/access.2024.3401851

[16] Usha, S., Geetha, P., Palanisamy, R., Kitmo, and Jember, Y.B. (2023) Analysis of Torque Controlling Strategies of Interior Permanent Magnet Synchronous Machine in Hybrid Electric Vehicle. *SN Applied Sciences*, **5**, Article No. 326. https://doi.org/10.1007/s42452-023-05563-w

[17] Premkumar, N., Madhavi, M.R., Kitmo, K. and Shanmugan, S. (2024) Utilizing the Lignocellulosic Fibers from Pineapple Crown Leaves Extract for Enhancing TiO_2 Interfacial Bonding in Dye-Sensitized Solar Cell Photoanodes. *Materials for Renewable and Sustainable Energy*, **13**, 13-25. https://doi.org/10.1007/s40243-023-00245-4

[18] Kitmo, Tchaya, G.B. and Djongyang, N. (2021) Optimization of the Photovoltaic Systems on the North Cameroon Interconnected Electrical Grid. *International Journal of Energy and Environmental Engineering*, **13**, 305-317. https://doi.org/10.1007/s40095-021-00427-8

[19] Sathyapriya, G., Natarajan, U., Sureshkumar, B., Navaneethakrishnan, G., Palanisamy, R. and Kitmo, (2024) Compliant Damper Development for Vibration Reduction in Turning of Aluminium. *Multiscale and Multidisciplinary Modeling, Experiments and Design*, **7**, 895-904. https://doi.org/10.1007/s41939-023-00253-x

[20] Sathyapriya, G., Natarajan, U., Sureshkumar, B., Navaneethakrishnan, G., Palanisamy, R., Aboras, K.M., *et al.* (2022) Development of Compliant Vibration Isolation Damper and Its Performance Analysis in Turning Operation. *Advances in Materials Science and Engineering*, **2022**, Article ID: 6860178. https://doi.org/10.1155/2022/6860178

[21] Bello-Pierre, N., Nisso, N., Kaoga, D.K., Kitmo and Tchakounté, H. (2023) Energy Efficiency in Periods of Load Shedding and Detrimental Effects of Energy Dependence in the City of Maroua, Cameroon. *Smart Grid and Renewable Energy*, **14**, 61-71. https://doi.org/10.4236/sgre.2023.144004

[22] Alphonse, S., Jacques, B., Kitmo, Djidimbele, R., Andre, P. and Cesar, K. (2021) Optimization PV/batteries System: Application in Wouro Kessoum Village Ngaoundere Cameroon. *Journal of Power and Energy Engineering*, **9**, 50-59. https://doi.org/10.4236/jpee.2021.911003

[23] Kitmo, Choudhury, S., Khan, A.A., Das, S. and Elnaggar, M.F. (2023) Intelligent Approach for Control Techniques Based on Complex Converter Structures. *International Journal of Energy Research*, **2023**, Article ID: 6770322. https://doi.org/10.1155/2023/6770322

[24] Babé, C., Kidmo, D.K., Tom, A., Mvondo, R.R.N., Boum, R.B.E. and Djongyang, N. (2020) Thermomechanical Characterization and Durability of Adobes Reinforced with Millet Waste Fibers (Sorghum Bicolor). *Case Studies in Construction Materials*, **13**, e00422. https://doi.org/10.1016/j.cscm.2020.e00422

[25] Babé, C., Kidmo, D.K., Tom, A., Mvondo, R.R.N., Kola, B. and Djongyang, N. (2021) Effect of Neem (Azadirachta Indica) Fibers on Mechanical, Thermal and Durability Properties of Adobe Bricks. *Energy Reports*, **7**, 686-698.

https://doi.org/10.1016/j.egyr.2021.07.085

[26] Harouna, B. (2011) Modélisation et mesure de propriétés thermiques d'un milieu-poreux humide: Brique de latérite avec gousse de mil. Ph.D. Thesis, Université-Cheik Anta Diop Dakar.